Received: 20 December 2019 | Revised: 7 February 2020 | Accepted: 24 February 2020

DOI: 10.1002/aoc.5649

Applied Organometallic Chemistry WILEY

FULL PAPER

A novel nanomagnetic solid acid catalyst for the synthesis of new functionalized bis-coumarin derivatives under microwave irradiations in green conditions

Zhila Zare-Akbari[1] | **Siavoush Dastmalchi**[2,3,4] | **Ladan Edjlali**[1] | **Leila Dinparast**[2] | **Moosa Es'haghi**[1]

[1]Department of Chemistry, Tabriz Branch, Islamic Azad University, Tabriz, Iran

[2]Biotechnology Research Center, Tabriz University of Medical Sciences, Tabriz, Iran

[3]School of Pharmacy, Tabriz University of Medical Sciences, Tabriz, Iran

[4]Faculty of Pharmacy, Near East University, Nicosia, North Cyprus, Turkey

Correspondence
Siavoush Dastmalchi, School of Pharmacy, Tabriz University of Medical Sciences, Tabriz, Iran.
Email: dastmalchi.s@tbzmed.ac.ir

In this study, a novel, green, environmentally friendly and magnetically heterogeneous catalyst based on the immobilization of sulfosalicylic acid onto Fe_3O_4 nanoparticles (Fe_3O_4@sulfosalicylic acid MNPs) is reported. The bis-coumarin analogs were synthesized in high yield using the reaction of 1 equivalent of aryl aldehydes with 2 equivalents of 4-hydroxycoumarin in water under microwave irradiation conditions. Scanning electron microscopy, transmission electron microscopy, energy-dispersive X-ray spectroscopy, X-ray diffraction, thermogravimetric analysis, dynamic light scattering, vibrating sample magnetometry, Fourier transform infrared spectroscopy, UV–visible absorption, and Brunauer-Emmett-Teller (BET) techniques confirmed the successful synthesis of the catalyst. The main attractive characteristics of the presented green protocol are very short reaction times (10–15 min), excellent yields, and the avoidance of hazardous or toxic reagent and solvents. Thermal durability, easy separation, and high reusability are important advantages of the new catalyst in comparison to other catalysts.

KEYWORDS

bis-coumarin, coumarin, green methodology, MNPs, sulfosalicylic acid

1 | INTRODUCTION

The coumarin ring as a heterocyclic compound has attracted a lot of attention in organic and medical chemistry.[1–3] Bis-coumarins are an important class of coumarin derivatives with considerable pharmacological and biological properties, such as antioxidant, anti-tumor, cytotoxicity, and anti-inflammatory properties.[4,5] These compounds are widely used in insecticidal, anti-fungal, anticoagulant, antihelminthic, and hypnotic agents, and also in HIV protease inhibition and phytoalexin, an as reducing and stabilizing agents and ligands.[4–9] Thus far, many bis-coumarin analogs have been discovered from natural sources,[10–13] including dicoumarol (*Melilotus alba*), gerberinol (*Gerbera lanuginose*), and ismailin (*Diospyros ismaili*) (Figure 1).

Several synthetic procedures have been used for the preparation of bis-coumarins.[14] The reactions of 4-hydroxycoumarin with (i) benzylic alcohols,[15] (ii) 1,2-diols,[16] and (iii) aromatic aldehydes are the most important protocols for these transformations. The last procedure is a direct method and has attracted special attention.[17] In recent years several catalytic systems have been reported for the synthesis of bis-coumarins using method (iii), for example molecular iodine,[18] tetramethyl guanidium,[19] Zn(proline)$_2$,[20] $POCl_3$ in dry dimethylformamide (DMF), phosphotungstic acid,[21] propane-1,2,3-triyltris,[22] ruthenium(III) chloride

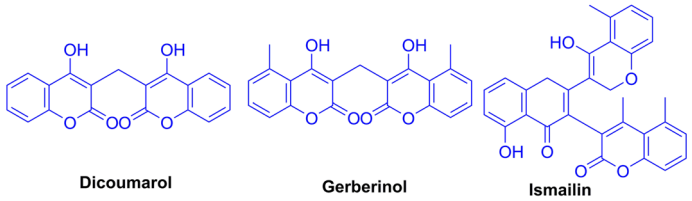

FIGURE 1 Some naturally occurring bis-coumarins

hydrate,[23] choline hydroxide,[24] sodium dodecyl sulfate,[25] silica sulfamic acid,[26] methane sulfonic acid,[27] sulfated titania,[28] and ethanol or acetic acid under reflux.[19] However, the present procedures suffer from one or more drawbacks, such as long reaction times, low yields, toxic residues, special apparatus, tedious work-up procedures, environmentally unfavorable solvents, and unreusability of catalysts.[29–33] Although homogeneous catalysts have considerable activity and selectivity in the different reaction mixtures, being separated from the reaction and applying large amounts of organic solvents are their most important disadvantages.[34–39]

Regarding the chemistry of sustainability, the development of humanitarian, environmentally friendly, and efficient synthetic procedures for the preparation of biologically active molecules both in terms of the selection of synthetic routes and the investigation of catalyst and solvent efficiency are significant challenges in organic synthesis.[34–36,40–43]

Nanomaterial utilization has been expanded due to their specific properties, for example surface modification ability, easy work-up, high surface area, high thermal and chemical durability, environmental friendliness, low cost, and simple isolation.[44–51] Organic molecules and complexes can be heterogenized on solid state nanomaterialsto provide support for catalyzing organic processes following the principles of green and sustainable chemistry.[34,38,52] In this method, minimum energy and reagents are used and minimum waste is generated.[34,36,37,53–55] Moreover, nanostructure supports are advantageous because they show higher reactivity and chemoselectivity than their corresponding bulk materials.[56–62] Moreover, surface modification of magnetic nanoparticles is an allowable method to eliminate the giant gap between homogeneous and heterogeneous catalysts.[63–67] Sulfuric acid is used as an efficient and irretrievable Brønsted–Lowry acid catalyst to generate different kinds of chemical materials.[68–71] Sulfonation with sulfosalicylic acid as a suitable, quick, and executable system has attracted great attention for the production of heterogeneous catalysts.[72] Hence, sulfuric acid coated magnetite nanoparticles as a new retrievable heterogeneous acid catalyst provides a new way to demonstrate a wonderful and efficacious system in order to simplify catalyst retrieval in various organic reactions.[73]

In this study, we report a green method to functionalize bis-coumarin analogues using aromatic aldehydes and 4-hydroxycoumarin in the presence of sulfosalicylic acid functionalized magnetic nanoparticle (MNP-sulfosalicylic acid) as a new, reusable, highly efficient, cost-effective, environmentally compatible, and biomedical catalytic system under microwave irradiation (180 W, maximum 60°C) in water with short reaction times and superb yields (Scheme 1).

2 | EXPERIMENTAL

2.1 | Synthesis of nanocatalyst Fe_3O_4@sulfosalicylic acid

The Fe_3O_4 magnetic nanoparticles were prepared by the coprecipitation technique as previously reported.[74] To prepare Fe_3O_4@sulfosalicylic acid, 1 g of the prepared Fe_3O_4 MNPs was dispersed in 100 ml of deionized water by sonication for 30 min. Afterwards, sulfosalicylic acid was added at a concentration of 50 mg/ml to the reaction mixture, which was stirred for 8 hr. Thereafter, the obtained MNPs were washed with deionized water a few times to eliminate excess sulfosalicylic acid, then the Fe_3O_4@sulfosalicylic acid MNPs were collected by magnet and dried under vacuum at 70°C for 12 hr.

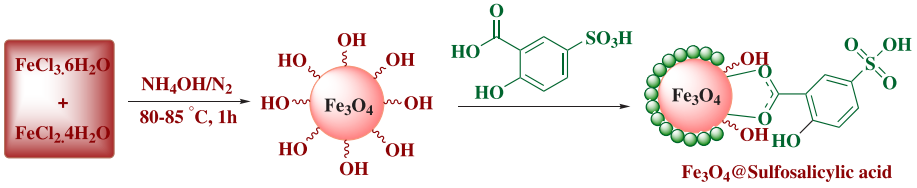

SCHEME 1 Synthesis of Fe_3O_4@sulfosalicylic acid

2.2 | General experimental procedure for the synthesis of bis-coumarin (1a–15a)

Fe_3O_4@sulfosalicylic acid (0.06 g) as catalyst was added to a mixture of aromatic aldehyde **1** (1 mmol) and 4-hydroxycoumarin **2** (2 mmol) in water (10 ml) and the obtained mixture was heated (maximum temperature 60°C) for specific times (Table 2) under microwave irradiation at 180 W. After completion of the reaction (monitored by TLC), hot ethanol as a diluting solvent was added to the reaction mixture and the Fe_3O_4@sulfosalicylic acid MNPs were collected from the reaction mixture by an external magnet. Finally, pure products ware obtained by recrystallization in ethanol.

2.3 | Spectral data

2.3.1 | 3,3′-(phenylmethylene) bis (4-hydroxy-2*H*-chromen-2-one (1a)

White solid. FT-IR, ν_{max} (KBr): 3434, 2968, 1696, 1506 cm^{-1}. ^1H NMR ($CDCl_3$, 400 MHz) δ: 8.30 (s, 1H, OH), 8.35 (s, 1H, OH), 6.87–7.89 (m, 13H, Ar–H), 6.09 (s, 1H, CH) ppm. ^{13}C NMR (DMSO, 100 MHz) δ: 162.71, 145.63, 141.82, 133.63, 131.10,128.92, 126.68, 123.93, 122.80, 116.45, 114.61, 113.42, 107.97, 36.41 ppm. HRMS [M + H] = *m*/*z*: 413.1645. Anal. calcd for $C_{25}H_{16}O_6$: C 72.81, H 3.91; found: C 72.76, H 3.87%.

2.3.2 | 3,3′-((4-nitrophenyl) methylene) bis(4-hydroxy-2*H*-chromen-2-one) (2a)

Light yellow solid. FT-IR, ν_{max} (KBr): 3438, 1682, 1595, 1505, 1380, 1138 cm^{-1}. ^{1} H NMR ($CDCl_3$, 400 MHz) δ: 8.20 (s, 1H, OH), 8.08 (s, 1H, OH), 6.96–7.71 (m, 12H, Ar–H), 6.19 (s, 1H, CH) ppm. ^{13}C NMR (DMSO, 100 MHz) δ: 169.32, 164.08, 155.35, 174.62, 144.63, 140.59, 130.24, 130.11, 126.85, 122.69, 120.42, 114.46, 112.77, 48.38 ppm. HRMS [M + H] = *m*/*z*: 458.0342. Anal. calcd for $C_{25}H_{15}NO_8$: C 65.65, H 3.31, N 3.06; found: C 65.60, H 3.30, N 3.29%.

2.3.3 | 3,3′-((4-ethoxyphenyl) methylene) bis(4-hydroxy-2*H*-chromen-2-one) (3a)

White solid. FT-IR, ν_{max} (KBr): 3375, 3161, 1716, 1573, 1402 cm^{-1}. ^1H NMR ($CDCl_3$, 400 MHz) δ: 1.37 (t, 3H, CH_3) 3.98 (q,2H, CH_2), 6.03 (s, 1H, CH), 6.82–7.63 (m, 12H, Ar–H),8.00 (s, 1H, OH), 8.04 (s, 1H, OH) ppm. ^{13}C NMR (DMSO, 100 MHz) δ: 165.83, 162.95, 155.35, 143.63, 140.59, 137.67, 130.24, 130.11, 126.85, 122.69, 120.42, 115.46, 112.77, 63.34, 37.65, 20.95 ppm. HRMS [M + H] = *m*/*z*: 457.0342. Anal. calcd for $C_{27}H_{20}O_7$: C 71.05, H 4.42; found: C 71.03, H 4.40%.

2.3.4 | 3,3′-((4-fluorophenyl) methylene) bis(4-hydroxy-2*H*-chromen-2-one) (4a)

White solid. FT-IR, ν_{max} (KBr): 3424, 1670, 1610, 1561, 1501, 1099 cm^{-1}. ^1H NMR ($CDCl_3$, 400 MHz) δ: 6.02 (s, 1H, CH),6.82–7.64 (m, 12H, Ar–H), 7.99 (s, 1H, OH), 8.04 (s, 1H, OH) ppm. ^{13}C NMR (DMSO, 100 MHz) δ: 162.87, 141.46, 137.15, 134.66,131.25, 130.90,129.17, 126.98, 122.40, 121.12,114.96, 112.98, 105.73 ppm. HRMS [M] = *m*/*z*: 521.3130. Anal. calcd for $C_{25}H_{15}FO_6$: C 69.77, H 3.51; found: C 69.75, H 3.50%.

2.3.5 | 3,3′-((4-bromophenyl) methylene) bis(4-hydroxy-2*H*-chromen-2-one) (5a)

White solid. FT-IR, ν_{max} (KBr): 3476, 2980, 1778, 1675, 1592, 1495, 1090, 770 cm^{-1}. ^1H NMR ($CDCl_3$, 400 MHz) δ: 6.10 (s, 1H, CH), 7.24–8.09(m, 12H, Ar–H), 8.16 (s, 1H, OH), 8.18 (s, 1H, OH) ppm.^{13}C NMR (DMSO, 100 MHz) δ: 164.83, 163.26, 158.10, 155.49, 141.89, 139.71, 131.61, 131.25, 126.43, 124.93, 121.09, 116.20, 113.96, 55.36 ppm. HRMS [M] = *m*/*z*: 504.0209. Anal. calcd for $C_{25}H_{15}BrO_6$: C 61.12, H 3.08; found: C 61.10, H 3.06%.

2.3.6 | 3,3′-((3-bromo-4-methoxyphenyl) methylene) bis(4-hydroxy-2*H*-chromen-2-one) (6a)

White solid. FT-IR, ν_{max} (KBr): 3438, 3054, 1683, 1612, 1507, 1440, 756 cm^{-1}. ^1H NMR ($CDCl_3$, 400 MHz) δ: 3.87 (s, 3H, OCH_3), 6.02 (s, 1H, CH) 6.82–7.64 (m, 11H, Ar–H), 7.99(s, 1H, OH), 8.05 (s, 1H, OH) ppm. ^{13}C NMR (DMSO, 100 MHz) δ: 164.58, 140.60, 133.91, 132.60, 132.14, 131.81, 127.18, 125.18, 121.84, 120.48, 112.96, 111.26, 105.73 ppm. HRMS [M] = *m*/*z*: 521.3130. Anal. calcd for $C_{26}H_{17}BrO_7$: C 59.90, H 3.29; found: C 59.87, H 3.28%.

2.3.7 | 3,3′-((4-methoxyphenyl) methylene) bis(4-hydroxy-2*H*-chromen-2-one) (7a)

White solid. FT-IR, ν_{max} (KBr): 3456, 2994, 1722, 1636 cm^{-1}. ^1H NMR ($CDCl_3$, 400 MHz) δ: 3.78 (s, 3H, OCH_3), 6.03 (s, 1H, CH), 6.82–7.63 (m, 12H, Ar–H),7.99 (s, 1H, OH), 8.04 (s, 1H, OH) ppm. ^{13}C NMR (DMSO, 100 MHz) δ: 164.83, 162.80, 158.35, 152.11, 147.87,

146.13, 132.88, 127.67, 126.43, 123.23, 123.09, 116.70, 114.50 ppm. HRMS [M + H] = *m*/*z*: 443.1645. Anal. calcd for $C_{26}H_{18}O_7$: C 70.58, H 4.10; found: C 70.55, H 4.07%.

2.3.8 | 3,3′-((3,4-dimethoxyphenyl) methylene) bis(4-hydroxy-2*H*-chromen-2-one) (8a)

White solid. FT-IR, ν_{max} (KBr): 3445, 3050, 1722, 1636 cm^{-1}. ^1H NMR ($CDCl_3$, 400 MHz) δ: 3.72 (s, 3H, OCH_3),3.85 (s, 3H, OCH_3), 6.06 (s, 1H, CH) 6.70–7.63 (m, 11H, Ar–H), 8.00 (s, 1H, OH), 8.05 (s, 1H, OH) ppm. ^{13}C NMR (DMSO, 100 MHz) δ: 164.58, 162.71, 150.37, 149.12, 141.81, 139.64, 138.65, 133.65, 127.67, 123.92, 122.79, 118.70, 114.62, 113.41, 111.72 ppm. HRMS [M + H] = *m*/*z*: 473.6214; Anal. calcd for $C_{27}H_{20}O_8$: C 68.64, H 4.27; found: C 68.60, H 4.24%.

2.3.9 | 3,3′-((2,3-dimethoxyphenyl) methylene) bis(4-hydroxy-2*H*-chromen-2-one) (9a)

White solid. FT-IR, ν_{max} (KBr): 3304, 2947, 1678, 1562 cm^{-1}. ^1H NMR (DMSO, 400 MHz) δ: 8.10 (s, 1H, OH), 8.04 (s, 1H, OH), 7.02–8.01 (m, 11H, Ar–H), 6.17 (s, 1H, CH), 3.86 (s, 3H, OCH_3), 3.56 (s, 3H, OCH_3) ppm. ^{13}CNMR (DMSO, 100 MHz) δ: 162.80, 161.09, 155.37, 142.64, 140.96, 132.88, 130.09, 125.93, 123.09, 119.94, 118.95, 114.50, 113.22, 111.96, 110.47, 59.85, 56.61, 33.66 ppm. HRMS [M + H] = *m*/*z*: 473.1945. Anal. calcd for $C_{27}H_{20}O_8$: C 68.64, H 4.27; found: C 68.60, H 4.24%.

2.3.10 | 3,3′-((2-chloro-4-fluorophenyl) methylene) bis(4-hydroxy-2*H*-chromen-2-one) (10a)

White solid. FT-IR, ν_{max} (KBr): 3441, 1696, 1594, 1558, 758 cm^{-1}. ^1H NMR ($CDCl_3$, 400 MHz) δ: 8.04 (s, 1H, OH), 7.98 (s, 1H, OH), 6.42–7.49 (m, 11H, Ar–H), 6.01 (s, 1H, CH) ppm. ^{13}C NMR (DMSO, 100 MHz) δ: 160.69, 160.60, 157.42, 152.36, 147.62, 146.63, 132.99, 132.66, 123.12, 119.90, 119.45, 116.92, 116.41, 50.62 ppm. HRMS [M + H] = *m*/*z*: 464.1414. Anal. calcd for $C_{25}H_{14}ClFO_6$: C 64.60, H 3.04; found: C 64.59, H 3.03%.

2.3.11 | 3,3′-((4-chlorophenyl) methylene) bis(4-hydroxy-2*H*-chromen-2-one) (11a)

White solid. FT-IR, ν_{max} (KBr): 3350, 2956, 1617, 1564 cm^{-1}. ^1H NMR ($CDCl_3$, 400 MHz) δ: 8.05 (s, 1H, OH), 7.99 (s, 1H, OH), 6.36–7.37 (m, 12H, Ar–H), 6.09 (s, 1H, CH) ppm. ^{13}C NMR (DMSO, 100 MHz) δ: 164.55, 163.50, 158.26, 151.97, 146.21, 141.57, 135.76, 129.96, 128.91, 128.41, 124.98, 116.13, 113.92 ppm. HRMS [M] = *m*/*z*: 460. 0814. Anal. calcd for $C_{25}H_{15}ClO_6$: C 67.20, H 3.38; found: C 67.17, H 3.87%.

2.3.12 | 3,3′-((5-nitrothiophen-2-yl) methylene) bis(4-hydroxy-2*H*-chromen-2-one) (12a)

Brown solid. FT-IR, ν_{max} (KBr): 3453, 2932, 1765, 1553 cm^{-1}. ^1H NMR ($CDCl_3$, 400 MHz): 10.41 (s, 1H, OH), 9.84 (s, 1H, OH), 6.88–7.51 (m, 10H, Ar–H), 4.85 (s, 1H, CH) ppm. δ ^{13}C NMR ($CDCl_3$, 100 MHz) δ: 160.65, 160.49, 152.61, 149.87, 148.93, 131.96, 129.29, 127.29, 124.63, 120.27, 119.07, 116.72, 115.14, 102.24, 37.24 ppm. MS [M] = *m*/*z*: 460.0814. Anal. calcd for $C_{23}H_{13}NO_8S$: C 59.61, H 2.83; found: C 60.07, H 3.01%.

2.3.13 | 3,3′-((5-bromofuran-2-yl) methylene) bis(4-hydroxy-2*H*-chromen-2-one) (13a)

Light brown solid. FT-IR, ν_{max} (KBr): 3445, 2951, 1722, 1559, 788 cm^{-1}. ^1H NMR ($CDCl_3$, 400 MHz) δ: 10.83 (s, 1H, OH), 9.79 (s, 1H, OH), 6.89–7.59 (m, 10H, Ar–H), 4.79 (s, 1H, CH) ppm. ^{13}C NMR ($CDCl_3$, 100 MHz) δ: 160.65, 160.49, 160.07, 156.07, 149.87, 127.9, 124.63, 122.50, 120.27, 119.07, 118.13, 116.72, 114.23, 101.35, 35.63 ppm. Anal. calcd for $C_{23}H_{13}BrO_7$: C 57.40, H 2.72; found: C 58.06, H 3.30; N 15.29%.

2.3.14 | 3,3′-((5-chlorothiophen-2-yl) methylene) bis(4-hydroxy-2*H*-chromen-2-one) (14a)

White solid. FT-IR, ν_{max} (KBr): 3430, 1676, 1559, 754 cm^{-1}. ^1H NMR ($CDCl_3$, 400 MHz) δ: 9.84 (s, 1H, OH), 9.66 (s, 1H, OH), 6.89–7.52 (m, 10H, Ar–H), 4.93 (s, 1H, CH) ppm. ^{13}C NMR ($CDCl_3$, 100 MHz) δ: 164.56, 163.18, 156.28, 141.34, 134.40,133.30, 129.29, 127.29, 126.18, 122.96, 116.72, 115.37, 105.72, 39.76 ppm. Calcd for $C_{23}H_{13}ClO_6S$: C 61.00, H 2.89; found: C 62.17; H 3.17%.

2.3.15 | 3,3′-((6-methylpyridin-2-yl) methylene) bis(4-hydroxy-2*H*-chromen-2-one) (15a)

Brown solid. FT-IR, ν_{max} (KBr): 3373, 2940, 1740, 1597 cm^{-1}. ^1H NMR ($CDCl_3$, 400 MHz) δ: 9.29 (s, 1H, OH), 9.88 (s, 1H, OH), 7.09–7.88 (m, 11H, Ar–H), 4.39 (s, 1H, CH), 2.39 (s, 1H, CH_3) ppm. ^{13}C NMR ($CDCl_3$,

100 MHz) δ: 162.95, 161.80, 157.66, 152.61, 138.59, 131.96, 131.84, 127.29, 123.19, 121.58, 120.27, 117.67, 104.80, 46.89, 29.65 ppm. Calcd for $C_{25}H_{17}NO_6$: C 70.25, H 4.01, N 3.28; found: C 67.17, H 3.87, N 2.98%.

3 | RESULTS AND DISCUSSION

3.1 | Preparation and characterization of Fe_3O_4@sulfosalicylic acid catalyst

In this study we report the synthesis of novel bis-coumarin derivatives using Fe_3O_4@sulfosalicylic acid MNPs as a novel nanocatalyst. Initially, the Fe_3O_4 MNPs were easily prepared in water by the co-precipitation method.[43] Then, sulfosalicylic acid catalyst was grafted onto the surface of the Fe_3O_4 MNPs by the reaction of its carboxylic acid functional groups with hydroxyl groups on the surface of the Fe_3O_4 MNPs in green condition (Scheme 1).

The structure of the Fe_3O_4@sulfosalicylic acid MNPs was characterized by various techniques: scanning electron microscopy (SEM), transmission electron microscopy (TEM), energy-dispersive X-ray spectroscopy (EDS), X-ray diffraction (XRD), thermogravimetric analysis (TGA), dynamic light scattering (DLS), vibrating sample magnetometry (VSM), Fourier transform infrared (FT-IR) spectroscopy, and UV–visible absorption (UV) analysis.

To evaluate the particle size and morphology of the synthesized Fe_3O_4@sulfosalicylic acid MNPs, SEM and TEM were performed. Figure 2 shows the SEM and TEM images of the uniform-sized particles with spherical shape with an average size of 55 and 50 nm, respectively. It is noticeable that the average diameter obtained from TEM is smaller than that obtained from SEM.

According to EDS results shown in Figure 3, the presence of Fe, O, C and S signals were verified. The results indicate that the iron oxide nanoparticles are functionalized by sulfosalicylic groups, and confirm the successfully synthesis of Fe_3O_4@sulfosalicylic acid MNPs.

To determine the crystalline structure of sulfosalicylic-coated MNPs, XRD was used (Figure 4). The XRD pattern of the Fe_3O_4@sulfosalicylic acid MNPs was found in the region 2θ = 20–80°. On the basis of Figure 4, the diffraction peaks located at 30.2°, 35.9°, 43.3°, 53.5°, 57.4°, 63.1°, and 74.5° correspond to the (220), (311), (400), (422), (511), (440), and (533) crystalline planes of the Fe_3O_4 structure, respectively (Fe_3O_4, reference Jcpds no, 82–1533). In addition, the crystalline size of Fe_3O_4@sulfosalicylic acid MNPs was estimated using the Scherrer equation from XRD pattern data to be 30 nm.

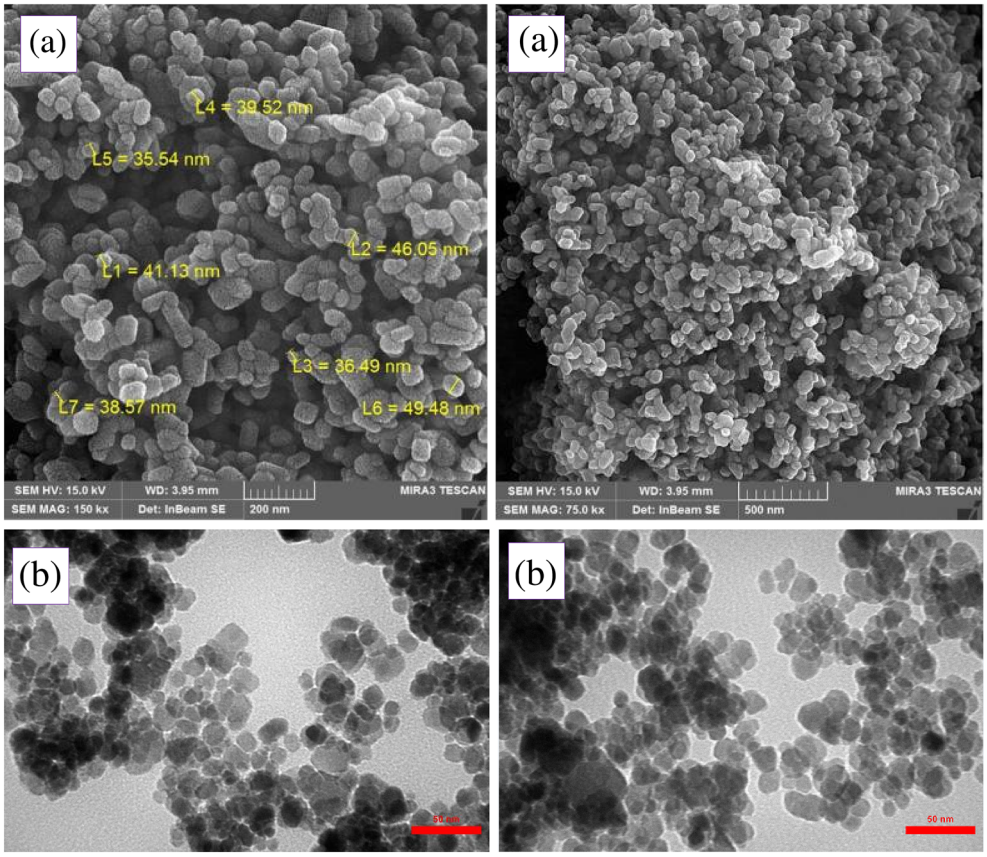

FIGURE 2 SEM and TEM images of Fe_3O_4@sulfosalicylic acid

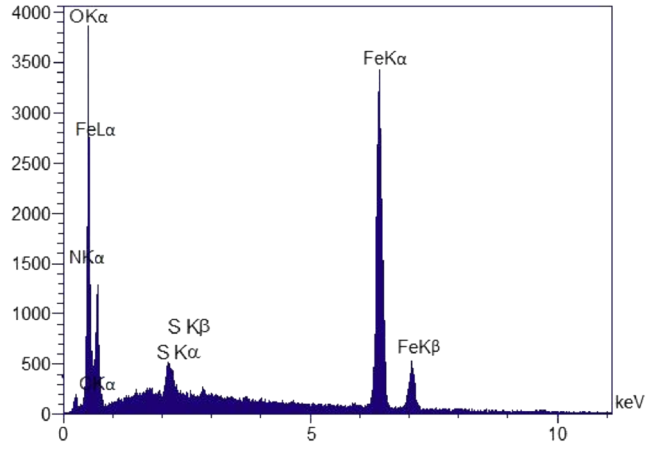

FIGURE 3 EDS spectrum of Fe_3O_4@sulfosalicylic acid

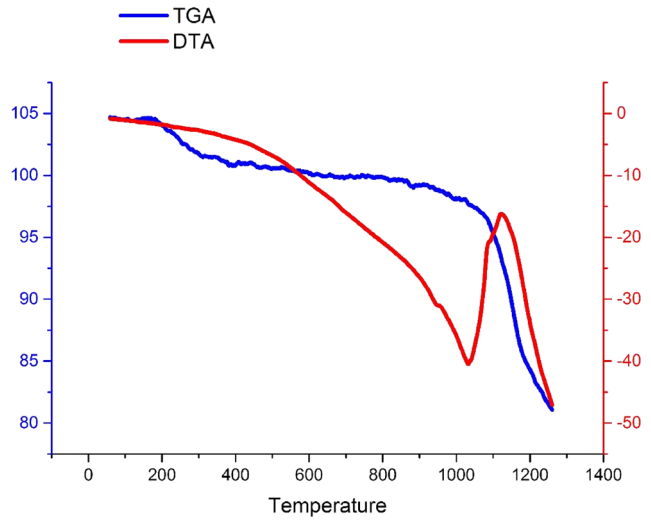

FIGURE 5 TGA spectra of the Fe_3O_4@sulfosalicylic acid

TGA was applied to determine the stability of the MNP-sulfosalicylic acid and the bonds formed between Fe_3O_4 and organic agent (sulfosalicylic acid). According to the TGA curve (Figure 5), the first weight loss below 100°C can be related to the solvent desorption and surface hydroxyl groups. The second weight loss can be ascribed to the decomposition of the sulfosalicylic acid grafted on the surface of the Fe_3O_4 MNPs. As can be seen from the TGA curve, the value of sulfosalicylic acid was measured to be about 6.5%.

DLS was used to estimate the zeta potential and particle size distribution of the Fe_3O_4@sulfosalicylic acid in an aqueous solution. According to the particle size distribution curves, the average particle size of Fe_3O_4@sulfosalicylic is 10 nm. In addition, the colloidal stability was evaluated on the basis of the zeta potential. Nanoparticles with zeta potential between −25 and +25 mV have a high degree of stability.[41] On the basis of Figure 6, Fe_3O_4@sulfosalicylic nanoparticles have high stability because the zeta potential of Fe_3O_4@sulfosalicylic acid in aqueous dispersion is −26.3 mV.

To evaluate the saturation magnetization of the Fe_3O_4 and Fe_3O_4@sulfosalicylic acid MNPs, VSM analysis was performed. According to Figure 7, the saturation magnetization for the Fe_3O_4@sulfosalicylic acid MNPs catalyst (45 emu/g) is less than that of the uncoated catalyst support (51 emu/g) which is due to the coated shell (sulfosalicylic acid).[44]

Figure 8 shows the FT-IR spectra of Fe_3O_4 MNPs, sulfosalicylic acid and Fe_3O_4 @sulfosalicylic acid MNPs. The FT-IR spectrum of the Fe_3O_4 MNPs demonstrates special absorption band peaks at 1615 and 585 cm^{-1}, which are attributed to the twisting vibration of the H–

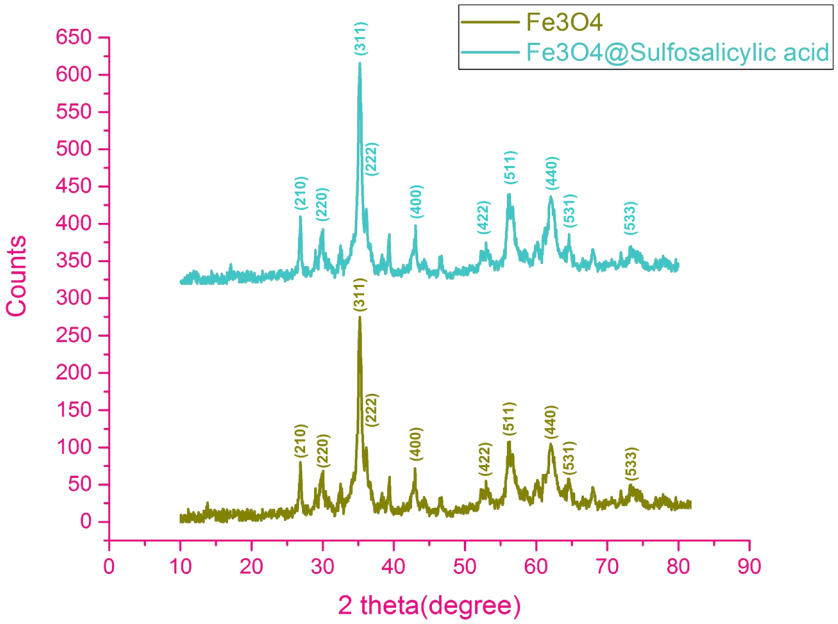

FIGURE 4 XRD diffraction pattern of Fe_3O_4@sulfosalicylic acid

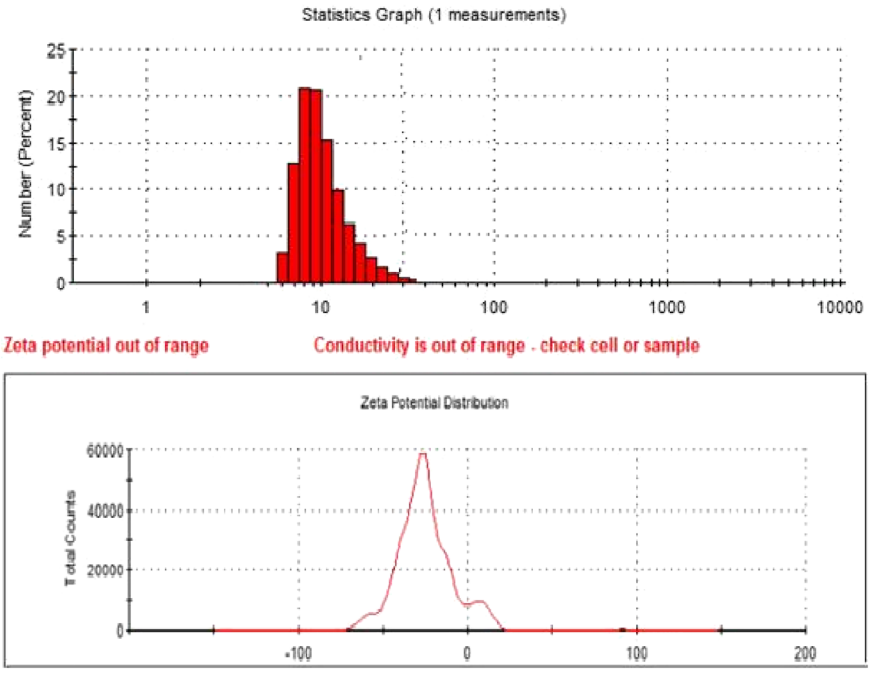

FIGURE 6 Particle size distribution (A) AND Zeta potential (B) of Fe_3O_4@sulfosalicylic acid

OH bond and the stretching vibration of the Fe–O bond on the surface of the support, respectively (Figure 8, black line). The red line in Figure 8 is the FT-IR spectrum of sulfosalicylic acid. It shows the O–H vibration band for 5-sulphosalicylic acid (3600–3200 cm^{-1}), which is observed at higher frequencies. The C–H stretching vibration of the aromatic is seen at 3060 cm^{-1} and the strong band at 1670 cm^{-1} is attributed to the O=C stretching of the carboxylic acid group. The symmetric and asymmetric stretching vibrations for SO_3 appear at 1121 and 1340 cm^{-1}, respectively.[45] The aromatic C–C stretching vibration, the O–H out-of-plane bending vibration, and the aromatic C–H out-of-plane bending vibration appear at 1608, 858, and 782 cm^{-1}, respectively.

The FT-IR spectrum of Fe_3O_4@sulfosalicylic acid is clearly different from those of sulfosalicylic acid (Figure 8, blue line) and Fe_3O_4 (Figure 8, black line). Regarding the sulfosalicylic acid functional group, the peaks at 585, 1011, 1718, and 3125 cm^{-1} are characteristic of the vibrations of Fe–O, C–O, COO–Fe, and C–H (stretching vibration) groups, respectively.

To characterize the conjugations of sulfosalicylic acid on the surface of the magnetic support, UV–Vis spectroscopy was performed. The UV–Vis absorption spectra of Fe_3O_4, sulfosalicylic acid, and Fe_3O_4@sulfosalicylic acid are depicted in Figure 9. The spectra show the characteristic absorption bands attributed to the usual p-p* and n-

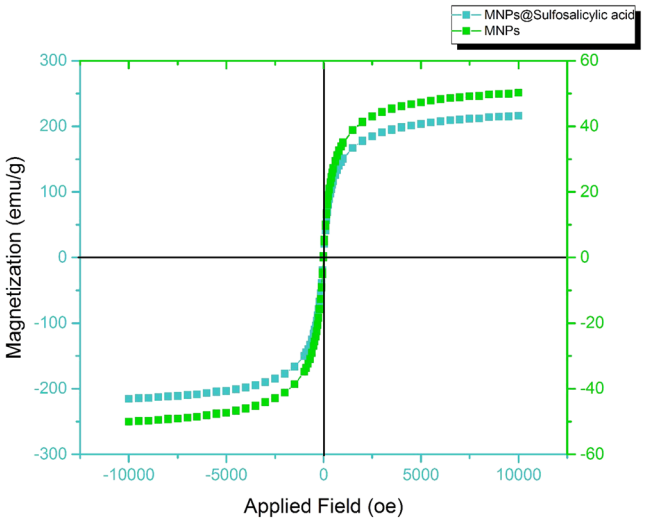

FIGURE 7 Magnetic diagram of Fe_3O_4@sulfosalicylic acid

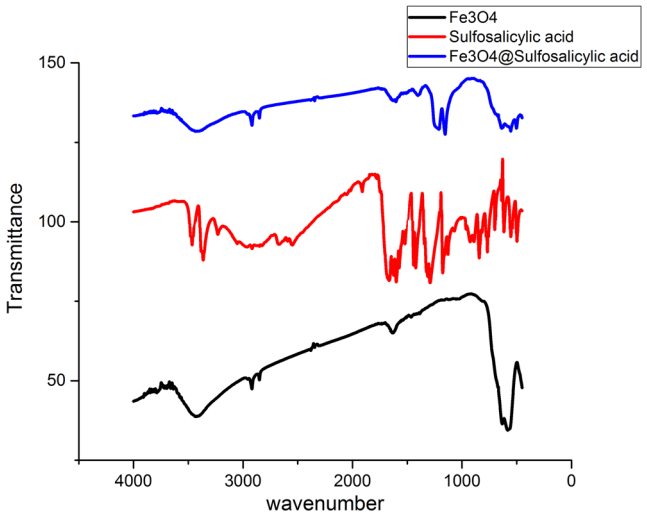

FIGURE 8 FT-IR spectra of sulfosalicylic acid, Fe_3O_4 MNPs, and Fe_3O_4@sulfosalicylic acid

p* transitions occurring in the 5-sulphosalicylate moieties of the salt, and the n-p* transition of the 5-sulphosalicylic acid (5SA), which is seen at 240 nm.[45] As shown in Figure 9, no characteristic UV–Vis peaks were observed for Fe_3O_4, but a peak at 240 nm was seen for Fe_3O_4@sulfosalicylic acid nanoparticles, which is in agreement with the standard sulfosalicylic acid UV–Vis spectrum. These results demonstrate the conjugation of sulfosalicylic acid on the surface of the Fe_3O_4 support.[45]

To measure the amount of loaded sulfosalicylic acid value on the surface of the catalyst, UV spectrophotometry at 240 nm was performed. Initially, various specific concentrations of sulfosalicylic acid, as a standard solution, were prepared. On the basis of the standard calibration curve, the amount of loaded sulfosalicylic acid was calculated (Figure 9). The quantity of sulfosalicylic acid grafted per 1 g of nanoparticles was determined to be about 0.97 mg.

BET can be regarded as an important analysis method for the measurement of the specific surface area of materials. The average particle diameter (nm) for particles with spherical morphology and narrow size distributions is calculated according to the formula:

$$\mathrm{dBET} = 6000/\tilde{c}ns$$

where s is the specific surface area in m^2/g and $\tilde{n}$ is the theoretical density in g/cm^3.[22] In surface area measurement, when particles do not join tightly together, nitrogen gas (N_2) can access most of the holes and surface area of the powder. A good measure of the real particle size independent of agglomeration is obtained. Thus, the surface area analysis result is close to the result obtained by TEM.[24] In this study, the specific surface area of the particles was found to be about 60.5 m^2/g and the calculated mean particle size (26 nm) was close to the TEM value (Figure 10). The results show that the powder contained particles with spherical shape as the gas accessed approximately the full surface area of the particles. The results obtained by BET, DLS, XRD, TEM, and SEM were shown in Table 1. The apparent differences between the results are due to the fact that different methods measure different property of the particle (e.g., projected area, surface area, volume and etc.) and hence, leading to the

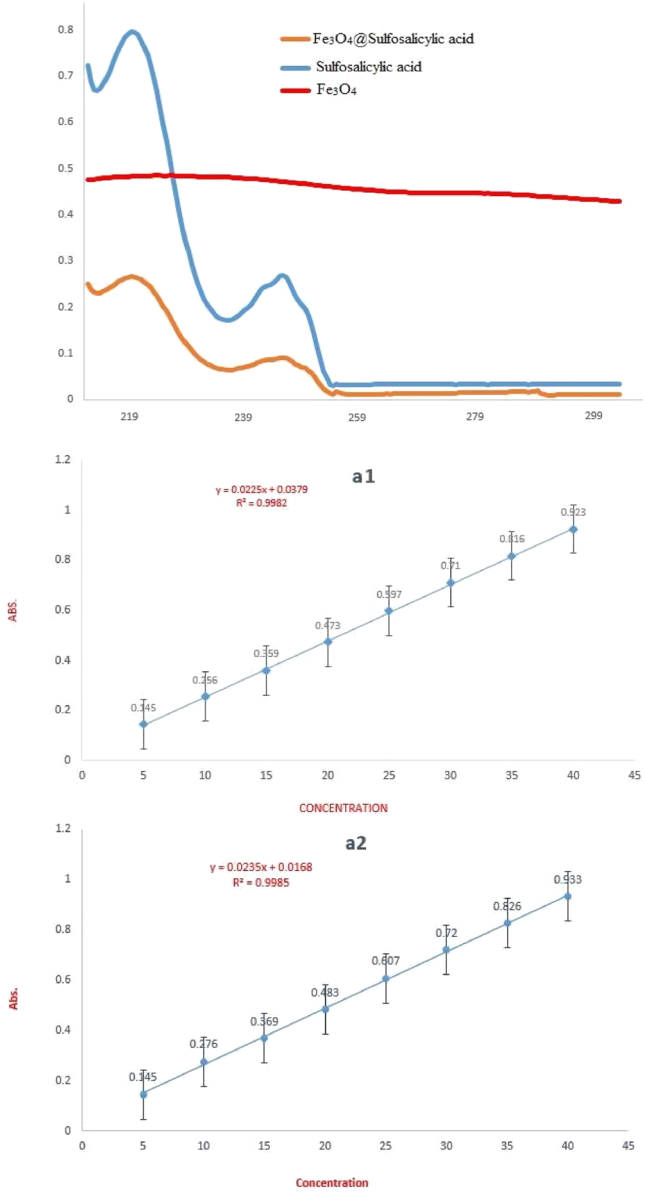

FIGURE 9 (a) UV–Vis spectra of sulfosalicylic acid, Fe_3O_4 MNPs and Fe_3O_4@sulfosalicylic acid

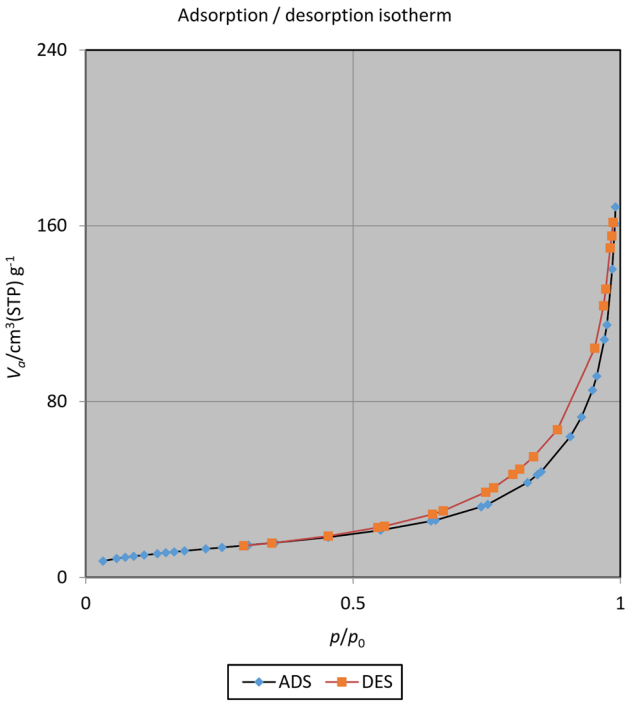

FIGURE 10 Nitrogen adsorption/desorption isotherms of Fe_3O_4@sulfosalicylic acid

TABLE 1 Fe_3O_4 @Sulfosalicylicacid MNPs obtained with TEM, SEM, XRD, BET, and DLS

Method	Mean diameter (nm)
TEM	50
SEM	55
BET	26
DLS	10
XRD	30

different result.[22] Table 1 presents the results of the different techniques used in this study.

4 | SYNTHESIS OF BIS-COUMARIN DERIVATIVES

On the basis of the importance of bis-coumarin derivatives, we decide to find a practical protocol with high yield. As the development of environmentally friendly and efficient synthetic methods is always desirable, we decided to investigate the possibility of preparing bis-coumarines by condensation of 4-hydroxycoumarin and arylaldehydes under microwave irradiation. To increase the yields and reduce the amount of waste materials and the reaction period, the effect of various reaction parameters was investigated. Accordingly, the effect of different reaction conditions, such as catalyst temperature, on the synthesis of compound **1a** by the condensation of benzaldehyde **1** (1 mmol) with 4-hydroxycoumarin **2** (2 mmol) as a model reaction was investigated and the results are summarized in Table 2. When the amount of Fe_3O_4@sulfosalicylic acid increased to more than 0.08 g, no significant improvement was observed. Moreover, when a smaller amount of catalyst (0.015 g) was used, the yield decreased. In addition, the reaction did not proceed efficiently in the absence of Fe_3O_4 @Sulfosalicylic acid MNPs even after 18 min. In this study, no other solvent was evaluated because of the green chemistry aim. The results show that the highest yield and lowest time of reaction were obtained when the reaction was carried out in the presence of 0.05 g of @sulfosalicylic acid MNPs under microwave irradiation at 180 W (maximum 60°C) in water as green solvent (Table 2, entry 9).

On the basis of this result, the scope of reactions was extended using a diverse range of aromatic aldehydes, as shown in Table 3. All the synthesized products were characterized by FT-IR, ^{1}H NMR, ^{13}CNMR, and melting points, comparing the results with those of the known compounds in the literature.

TABLE 2 Optimization of the model reaction of compound **1a**[aa]

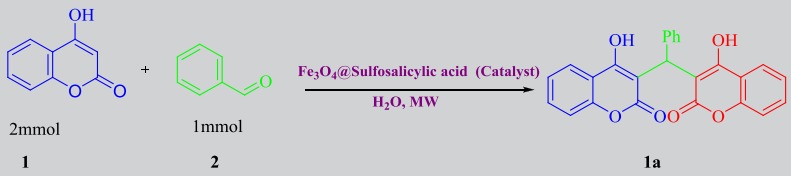

Entry	Catalyst (g)	Power[bb]	Time (min)	Yield (%)[cc]
2	Sulfosalicylic acid (0.01)	180	15	75
3	$FeCl_3.6H_2O$ (0.05)	180	15	43
4	Bulk-Fe_3O_4 (0.05)	180	15	50
5	Nano-Fe_3O_4 (0.05)	180	15	68
6	Fe_3O_4@sulfosalicylic acid (0.03)	180	20	89
7	Fe_3O_4@sulfosalicylic acid (0.03)	300	10	92
8	Fe_3O_4@sulfosalicylic acid (0.05)	100	10	89
9	Fe_3O_4@sulfosalicylic acid (0.05)	180	10	96
10	Fe_3O_4@sulfosalicylic acid (0.08)	180	10	96
11	Fe_3O_4@sulfosalicylic acid (0.015)	180	10	80
12	-	180	20	30

[a]The reaction was carried out under microwave irradiation conditions in water.
[b]The reaction was tested at different microwave powers (100–300 W) at range of 50–100°C.
[c]Isolated yields.

The structures of all the novel compounds were determined using FT-IR, ^{1}H NMR, ^{13}C NMR, and elemental analysis. The mass spectra of these compounds displayed molecular ion peaks at the appropriate *m/z* values.

The suggested reaction mechanism for the described combination is depicted in Scheme 2 based on the previously reported reaction pathway.[24,76] The reaction can be visualized as proceeding through a Knoevenagel condensation product as the key intermediate. In this step, the catalyst plays an important role in the condensation of the activated aldehyde (by the acid catalyst) with the 4-hydroxycoumarin to give an α,β-unsaturated intermediate. Finally, the catalyst also plays a significant role in the Michael addition of the second 4-hydroxycoumarin with an α,β-unsaturated intermediate to give the final polyhydroquinoline product. Finally, a tautomeric proton shift produces the final bis-coumarin product (Scheme 2).

The reusability and recoverability are two main advantages of the nanocatalysts. Thus, in this regard we checked the recyclability of the MNPs@sulfosalicylic acid under microwave irradiation (180 W, maximum 60°C) in water using a selected model of 4-hydroxycoumarin and benzaldehyde in the presence of MNPs@sulfosalicylic acid (Table 2, entry 1).

To isolate the catalyst from the reaction mixture after completion of the reaction, the reaction mixture was diluted with hot ethanol and the solid catalyst was removed using an external magnet, washed with the same solvent several times, dried at room temperature, and reused in the next similar reaction. According to Figure 11, the recovered catalyst was used for six continuous cycles without any significant deterioration of its catalytic activity. MNP-modified catalyst is readily suspended in ethanol and separated from the reaction mixture. This separation approach is not time-consuming in comparison to standard methods such as centrifugation and filtration.

After using the catalyst, the stability of the recovered Fe_3O_4 @Sulfosalicylic acid MNPs was characterized by TEM, SEM, VSM, FT-IR, DLS, EDS, UV–Vis, and XRD (Figure 12). The results show good agreement with the fresh catalyst analysis.

In addition, we evaluated the effect of the diverse power of microwave irradiation on the stability of sulfosalicylic acid in the MNPs@sulfosalicylic acid. As

TABLE 3 Synthesis of bis-coumarin derivatives in Fe_3O_4 @Sulfosalicylic acid MNPs (0.05 g) as catalyst under microwave irradiation (180 W, maximum 60°C) in water

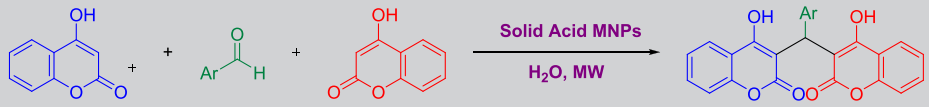

Entry	R^1	Product	Time (min)	Yield (%)[aa]	MP (obs.) (°C)	MP (lit.) (°C)
1	Ph-CHO	**1a**	10	94	228–230	230–231[75]
2	4-$NO_3C_6H_4$	**2a**	17	95	234–236	232–233[75]
3	4-$C_2H_5OC_6H_4$	**3a**	10	92	214–215	212–214[75]
4	4-FC_6H_4	**4a**	10	94	215–217	214–216[75]
5	4-BrC_6H_4	**5a**	10	88	265–267	266–268[75]
6	4-CH_3O,5BrC_6H_3	**6a**	12	90	242–244	241–243[75]
7	4-$CH_3OC_6H_4$	**7a**	14	87	250–252	251–252[75]
8	4,5-$CH_3OC_6H_3$	**8a**	10	73	245–247	264–266[75]
9	2,3-$CH_3OC_6H_3$	**9a**	10	92	259–260	255–257[75]
10	4-F, 2-ClC_6H_3	**10a**	10	89	256–258	255–257[75]
11	4-ClC_6H_4	**11a**	12	86	259–261	260–261[75]
12	5-NO_3, 2-thiophene	**12a**	15	90	187–189	Present work
13	5-Br, 2-furaldehyde	**13a**	10	85	178–180	Present work
14	5-Cl, 2-thiophene	**14a**	10	93	254–257	Present work
15	5-CH_3, 2-pyridine	**15a**	10	91	230–232	Present work

[a]Isolated yield.

SCHEME 2 Proposed mechanism for the synthesis of bis-coumarin derivatives

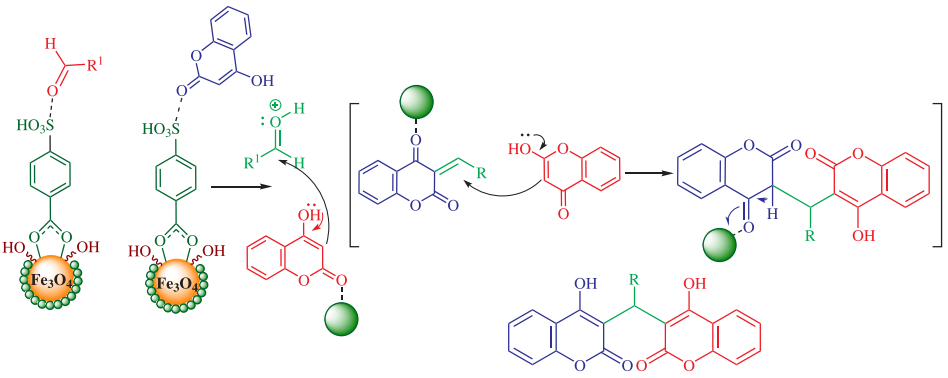

FIGURE 11 Reusability of Fe_3O_4@sulfosalicylic acid

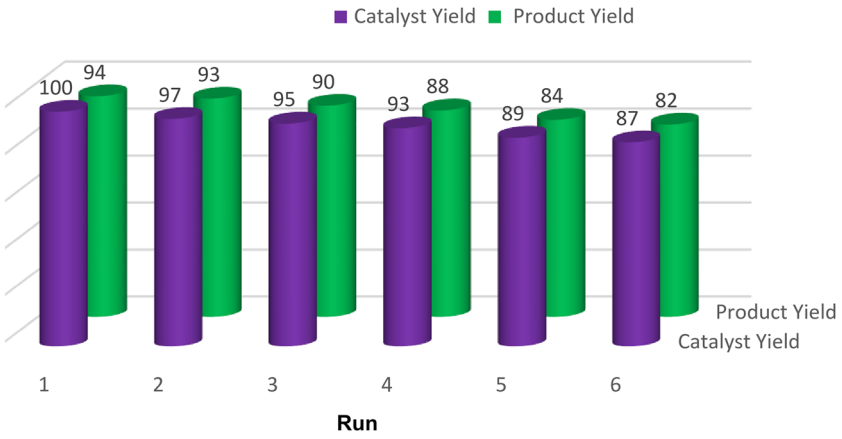

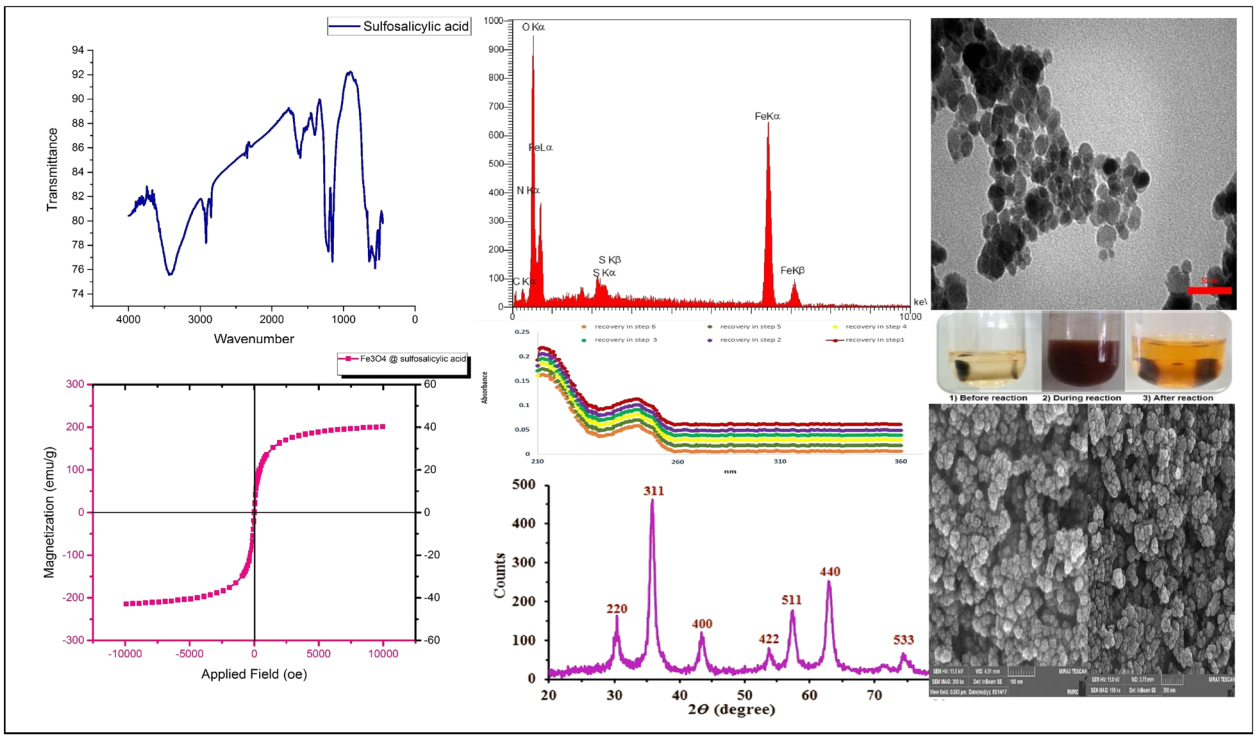

FIGURE 12 TEM, SEM, FT-IR, DLS, EDS, UV–Vis, XRD, and VSM analysis of spent Fe_3O_4@sulfosalicylic acid

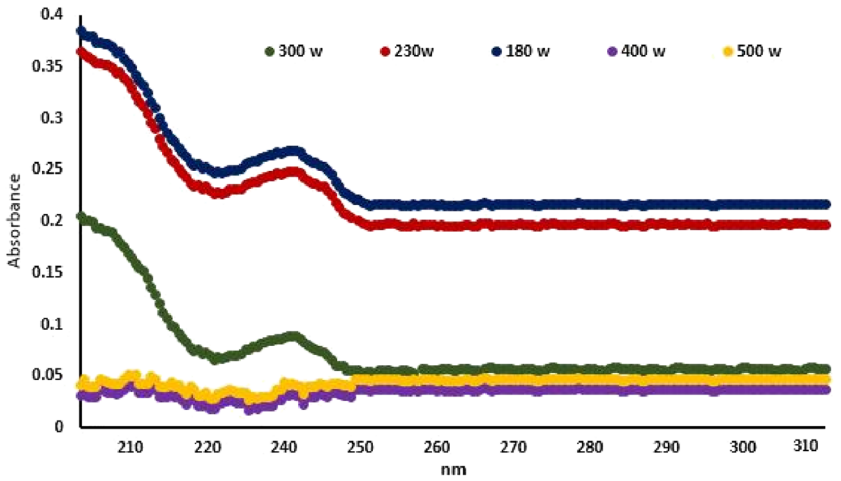

FIGURE 13 Effect of various powers of microwave irradiation on Fe_3O_4@sulfosalicylic acid

TABLE 4 Comparison of the efficiency of Fe_3O_4 @Sulfosalicylic acid MNPs with previously reported methods

Entry	Catalyst/condition	Time (min)	Yield (%)[aa]	Ref.
1	Ionic liquids, reflux	260 min	84	Previous work[75]
2	Choline hydroxide, reflux	240 min	86	Previous work[24]
3	No catalyst/trifluoroethanol, reflux	360 min	80	Previous work[19]
4	Fe_3O_4@sulfosalicylic acid/H_2O, MW[bb] (180 W, maximum 60°C)	10 min	96	Present work

[a]Isolated yield.
[b]The reaction was carried out under microwave irradiation conditions.

can be seen from Figure 13, the presence of sulfosalicylic acid on the surface of the MNPs decreases with the increasing power of microwave irradiation. Moreover, the absence of peaks at 240 nm proves the non attendance of the sulfosalicylic acid at 400 and 500 W.

Table 4 shows the results from the synthesis of bis-coumarin by reaction of benzaldehyde and 4-hydroxycoumarin in the presence of Fe_3O_4 @Sulfosalicylic acid MNPs which has been compared to the previously reported procedures. The results show that the present method is preferable because of its reaction times and efficiency.

5 | CONCLUSIONS

Sulfosalicylic acid was supported on the surface of Fe_3O_4 MNPs via a one-step green procedure. Its structure was fully characterized by TEM, SEM, XRD, UV–Vis, EDS, FT-IR, DLS, and VSM analysis. The as-prepared heterogenized solid acid catalyst was used as an efficient catalytic system for the synthesis of bis-coumarin derivatives in aldehydes and 4-hydroxycoumarin under microwave irradiation and green conditions. This environmentally friendly catalytic system displays excellent green chemistry properties, such as nontoxic reagents, short reaction time, excellent yields, avoidance of by-products and hazardous organic solvents, recyclability, and easy workup.

ACKNOWLEDGEMENTS

The authors wish to express their special thanks to Dr. Malihe Akhavan from University of Tehran North Branch, Islamic Azad University, Tehran, Iran. Part of this work was connected to the Ph.D. Thesis of Zhila Zare Akbari from Tabriz Branch, Islamic Azad University. The authors thank the Mazandaran University of Medical Sciences for providing laboratory facilities to carry out this research.

ORCID

Zhila Zare-Akbari https://orcid.org/0000-0002-7657-7493
Siavoush Dastmalchi https://orcid.org/0000-0001-9427-0770

REFERENCES

[1] M. Gaber, N. El-Wakiel, K. El-Baradie, S. Hafez, *J. Iran. Chem. Soc.* **2019**, *16*(1), 169.
[2] R. Tayebee, A. Pejhan, H. Ramshini, B. Maleki, N. Erfaninia, Z. Tabatabaie, E. Esmaeili, *Appl. Organomet. Chem.* **2018**, *32*(1), e3924.

[3] W. S. Hamama, M. E. Ibrahim, A. E. Metwalli, H. H. Zoorob, *Res. Chem. Intermed.* **2017**, *43*(11), 5943.
[4] S. Hamulakova, M. Kozurkova, K. Kuca, *Curr. Org. Chem.* **2017**, *21*(7), 602.
[5] Q. Ren, C. Gao, Z. Xu, Y. Xu, M. Liu, X. Wu, J.-G. Guan, L. Feng, *Curr. Top. Med. Chem.* **2018**, *18*(2), 101.
[6] B. Maleki, *Org. Prep. Proced. Int.* **2016**, *48*(3), 303.
[7] U. Salar, A. Nizamani, F. Arshad, K. M. Khan, M. I. Fakhri, S. Perveen, N. Ahmed, M. I. Choudhary, *Bioorg. Chem.* **2019**, *91*, 103170.
[8] D. Shahzad, A. Saeed, M. Faisal, F. A. Larik, S. Bilquees, P. A. Channar, *Org. Prep. Proced. Int.* **2019**, *51*(3), 199.
[9] N. O. Mahmoodi, Z. Jalalifard, G. P. Fathanbari, *J. Chin. Chem. Soc.* **2020**, *67*(1), 172.
[10] D. Yu, M. Suzuki, L. Xie, S. L. Morris-Natschke, K.-H. Lee, *Med. Res. Rev.* **2003**, *23*(3), 322.
[11] A. Detsi, C. Kontogiorgis, D. Hadjipavlou-Litina, *Expert Opin. Ther. Pat.* **2017**, *27*(11), 1201.
[12] M. Kumar, R. Singla, J. Dandriyal, V. Jaitak, *Anti-Cancer Agents Med. Chem.* **2018**, *18*(7), 964.
[13] D. Cao, Z. Liu, P. Verwilst, S. Koo, P. Jangjili, J. S. Kim, W. Lin, *Chem. Rev.* **2019**, *119*(18), 10403.
[14] P. Teli, A. Sethiya, S. Agarwal, *ChemistrySelect* **2019**, *4*(47), 13772.
[15] A. Montagut-Romans, M. Boulven, M. Lemaire, F. Popowycz, *New J. Chem.* **2014**, *38*(4), 1794.
[16] S. K. Patil, D. V. Awale, M. M. Vadiyar, S. A. Patil, S. C. Bhise, S. S. Kolekar, *Res. Chem. Intermed.* **2017**, *43*(10), 5365.
[17] S. A. Mayank, P. Raj, R. Kaur, A. Singh, N. Kaur, N. Singh, *New J. Chem.* **2017**, *41*(10), 3872.
[18] M. Kidwai, V. Bansal, P. Mothsra, S. Saxena, R. K. Somvanshi, S. Dey, T. P. Singh, *J. Mol. Catal. A: Chem.* **2007**, *268*(1–2), 76.
[19] A. Zhu, M. Wang, L. Li, J. Wang, *RSC Adv.* **2015**, *5*(90), 73974.
[20] Z. N. Siddiqui, F. Farooq, *Catal. Sci. Technol.* **2011**, *1*(5), 810.
[21] P. Singh, P. Kumar, A. Katyal, R. Kalra, S. K. Dass, S. Prakash, R. Chandra, *Catal. Letters* **2010**, *134*(3–4), 303.
[22] M. A. Zolfigol, N. Bahrami-Nejad, F. Afsharnadery, S. Baghery, *J. Mol. Liq.* **2016**, *221*, 851.
[23] B. Akhlaghinia, P. Sanati, A. Mohammadinezhad, Z. Zarei, *Res. Chem. Intermed.* **2019**, *45*(5), 3215.
[24] A. Zhu, S. Bai, L. Li, M. Wang, J. Wang, *Catal. Letters* **2015**, *145*(4), 1089.
[25] H. Mehrabi, H. Abusaidi, *J. Iran. Chem. Soc.* **2010**, *7*(4), 890.
[26] K. Niknam, S. A. Sajadi, R. Hosseini, M. Baghernejad, *Iran. J. Catal.* **2014**, *4*(3), 163.
[27] X. Qi, M.-W. Xue, X.-J. Sun, Y. Zhi, J.-F. Zhou, *Res. Chem. Intermed.* **2014**, *40*(3), 1187.
[28] B. Karmakar, A. Nayak, J. Banerji, *Tetrahedron Lett.* **2012**, *53*(33), 4343.
[29] F. Shirini, M. P. Lati, *J. Iran. Chem. Soc.* **2017**, *14*(1), 75.
[30] L. G. de Souza, M. N. Rennã, J. D. Figueroa-Villar, *Chem.-Biol. Interact.* **2016**, *254*, 11.
[31] E. Kolvari, N. Koukabi, A. Khoramabadi-zad, A. Shiri, M. Zolfigol, *Curr. Org. Synth.* **2014**, *10*(6), 837.
[32] M. A. Zolfigol, A. Khazaei, F. Karimitabar, M. Hamidi, *Appl. Sci.* **2016**, *6*(1), 1.
[33] I. Kostova, *Curr. Med. Chem. Agents* **2005**, *5*(1), 29.
[34] A. Ghorbani-Choghamarani, M. Mohammadi, R. H. E. Hudson, T. Tamoradi, *Appl. Organomet. Chem.* **2019**, *33*(8), e4977.
[35] L. Chen, A. Noory Fajer, Z. Yessimbekov, M. Kazemi, M. Mohammadi, *J. Sulfur Chem.* **2019**, *40*(4), 451.
[36] A. Ghorbani-Choghamarani, M. Mohammadi, Z. Taherinia, *Chem. Soc.* **2019**, *16*(2), 411.
[37] Q. Pu, M. Kazemi, M. Mohammadi, *Mini. Rev. Org. Chem.* **2019**, *16*(9), 5775.
[38] A. Ghorbani-Choghamarani, M. Mohammadi, T. Tamoradi, M. Ghadermazi, *Polyhedron* **2019**, *158*, 25.
[39] M. Kazemi, S. M. Nasr, Z. Chen, M. Mohammadi, *Mini. Rev. Org. Chem.* **2019**, *16*, 1.
[40] B. Jiang, T. Rajale, W. Wever, S. J. Tu, G. Li, *Chem.-an Asian J.* **2010**, *5*(11), 2318.
[41] S. Rahmani, B. Zeynizadeh, *Res. Chem. Intermed.* **2019**, *45*(3), 1227.
[42] S. Agarwal, D. Agarwal, D. Gandhi, K. Goyal, P. Goyal, *Lett. Org. Chem.* **2018**, *15*(10), 863.
[43] D. Gandhi, S. Agarwal, *J. Heterocycl. Chem.* **2018**, *55*(12), 2977.
[44] M. Kazemi, L. Shiri, *Mini. Rev. Org. Chem.* **2017**, *15*(2), 86.
[45] S. Chaturvedi, P. N. Dave, N. K. Shah, *J. Saudi Chem. Soc.* **2012**, *16*(3), 307.
[46] C. W. Lim, I. S. Lee, *Nano Today* **2010**, *5*(5), 412.
[47] M. Kazemi, M. Mohammadi, *Appl. Organomet. Chem.* **2020**, *34*(3), e5400.
[48] A. Ghorbani-Choghamarani, M. Mohammadi, L. Shiri, Z. Taherinia, *Res. Chem. Intermed.* **2019**, *45*(11), 5705.
[49] T. Tamoradi, S. M. Mousavi, M. Mohammadi, *New J. Chem.* **2020**, *44*(7), 3012.
[50] M. Mohammadi, A. Ghorbani-Choghamarani, *New J. Chem.* **2020**, *44*(7), 2919.
[51] M. Nikoorazm, M. Khanmoradi, M. Mohammadi, *Appl. Organomet. Chem.* **2020**, e5504.
[52] M. K. Rofouei, A. Aghaei, *J. Iran. Chem. Soc.* **2013**, *10*(5), 969.
[53] I. Del Hierro, Y. Pérez, M. Fajardo, *Appl. Organomet. Chem.* **2016**, *30*(4), 208.
[54] J. Xia, X. Huang, S. You, M. Cai, *Appl. Organomet. Chem.* **2019**, *33*(8), e5001.
[55] N. Azizi, E. Farhadi, *Appl. Organomet. Chem.* **2018**, *32*(3), e4188.
[56] M. Kazemi, M. Ghobadi, A. Mirzaie, *Nanotechnol. Rev.* **2018**, *7*(1), 43.
[57] S. A. Jadhav, A. P. Sarkate, A. V. Raut, D. B. Shinde, *Res. Chem. Intermed.* **2017**, *43*(8), 4531.
[58] C. T. Ma, J. J. Wang, A. D. Zhao, Q. L. Wang, Z. H. Zhang, *Appl. Organomet. Chem.* **2017**, *31*(12), e3888.
[59] d. arefeh, M. R. Naimi-Jamal, F. Matloubi Moghaddam, S. E. Ayati. Nitro compound reduction in the presence of robust palladium immobilized on modified magnetic Fe_3O_4 nanoparticles as a recoverable catalyst. In: Proc. 21st Int. Electron. Conf. Synth. Org. Chem., vol. 32. Basel, Switzerland: MDPI 2017; 4825.
[60] F. Manouchehri, B. Sadeghi, F. Najafi, M. H. Mosslemin, *J. Iran. Chem. Soc.* **2018**, *15*(8), 1673.
[61] S. M. Sadeghzadeh, R. Zhiani, S. Emrani, *Appl. Organomet. Chem.* **2018**, *32*(3), e4130.
[62] H. Sharghi, I. Ghaderi, M. M. Doroodmand, *Appl. Organomet. Chem.* **2017**, *31*(12), 11550.

[63] S. Sajjadifar, Z. Gheisarzadeh, *Appl. Organomet. Chem.* **2019**, *33*(1), e4602.
[64] M. Rajabzadeh, H. Eshghi, R. Khalifeh, M. Bakavoli, *Appl. Organomet. Chem.* **2018**, *32*(2), e4052.
[65] T. K. Khatab, A. M. Abdelghany, H. A. Soliman, *Appl. Organomet. Chem.* **2019**, *33*(5), e4783.
[66] Y. Hu, Y. Yang, R. Fan, K. Lin, D. Hao, D. Xia, P. Wang, *Appl. Organomet. Chem.* **2019**, *33*(9), e5060.
[67] N. Iranpoor, H. Firouzabadi, A. Rostami, *Appl. Organomet. Chem.* **2013**, *27*(9), 501.
[68] S. Moradi, M. A. Zolfigol, M. Zarei, D. A. Alonso, A. Khoshnood, A. Tajally, *Appl. Organomet. Chem.* **2018**, *32*(2), e4043.
[69] T. Shamsi, A. Amoozadeh, S. M. Sajjadi, E. Tabrizian, *Appl. Organomet. Chem.* **2017**, *31*(7), e3636.
[70] M. Ma, Y. Yang, R. Feng, L. Jia, G. Chen, W. Li, P. Lyu, *Appl. Organomet. Chem.* **2018**, *32*(12), e4534.
[71] H. Hassani, M. A. Nasseri, B. Zakerinasab, F. Rafiee, *Appl. Organomet. Chem.* **2016**, *30*(6), 408.
[72] A. Pramanik, R. Roy, S. Khan, A. Ghatak, S. Bhar, *Tetrahedron Lett.* **2014**, *55*(10), 1771.
[73] H. Naeimi, Z. S. Nazifi, *Appl. Catal. A Gen.* **2014**, *477*, 132.
[74] M. A. Ashraf, Z. Liu, W.-X. Peng, C. Gao, *Catal. Letters* **2020**, *150*(3), 683.
[75] A. N. Nadaf, K. Shivashankar, *J. Heterocycl. Chem.* **2018**, *55*(6), 1375.
[76] D. Cao, Z. Liu, P. Verwilst, S. Koo, P. Jangili, J. S. Kim, W. Lin, *Chem. Rev.* **2019**, *119*(18), 10403. *Chem. Rev.* **2019**, *119*(21), 11550.

How to cite this article: Zare-Akbari Z, Dastmalchi S, Edjlali L, Dinparast L, Es'haghi M. A novel nanomagnetic solid acid catalyst for the synthesis of new functionalized bis-coumarin derivatives under microwave irradiations in green conditions. *Appl Organometal Chem*. 2020;e5649. https://doi.org/10.1002/aoc.5649